Journal Pre-proofs

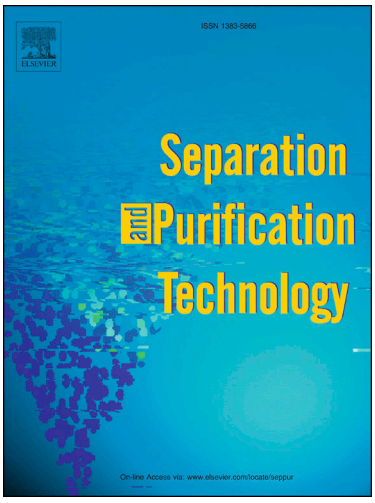

A more appropriate way to optimize the hybrid reactive-extractive distillation system

Eduardo Sánchez-Ramírez, Shirui Sun, Jia Yi Sim, Ao Yang, Zong Yang Kong, Juan Gabriel Segovia-Hernández

PII: S1383-5866(24)00923-7
DOI: https://doi.org/10.1016/j.seppur.2024.127184
Reference: SEPPUR 127184

To appear in: *Separation and Purification Technology*

Received Date: 17 January 2024
Revised Date: 6 March 2024
Accepted Date: 19 March 2024

Please cite this article as: E. Sánchez-Ramírez, S. Sun, J.Y. Sim, A. Yang, Z.Y. Kong, J.G. Segovia-Hernández, A more appropriate way to optimize the hybrid reactive-extractive distillation system, *Separation and Purification Technology* (2024), doi: https://doi.org/10.1016/j.seppur.2024.127184

A more appropriate way to optimize the hybrid reactive-extractive distillation system

Eduardo Sánchez-Ramírez[1], Shirui Sun[2], Jia Yi Sim[3], Ao Yang[4], Zong Yang Kong[3,*], Juan Gabriel Segovia-Hernández[1,*]

[1]Universidad de Guanajuato, Campus Guanajuato, División de Ciencias Naturales y Exactas, Departamento de Ingeniería Química, Noria Alta s/n, 36050, Guanajuato, Gto, Mexico

[2]School of Chemistry and Chemical Engineering, Yangtze Normal University, 408100, China

[3]Department of Engineering, School of Engineering and Technology, Sunway University, Bandar Sunway 47500, Selangor, Malaysia

[4]College of Safety Engineering, Chongqing University of Science & Technology, Chongqing 401331, P.R. China

Abstract

Existing studies on reactive-extractive distillation (RED) commonly misapply optimization variables by including reaction stages. Given the uncatalyzed nature of ethylene oxide (EO) hydration in RED, where it naturally occurs throughout the column, a more appropriate strategy is to optimize only the total stages, allowing the reactive stage to align accordingly. However, previous attempts to implement this approach faced challenges. Here we introduce an algorithm addressing the variable overlap issue in optimizing RED, exemplified in two case studies. In Case 1, we explored a distinct scenario where the original process designated a specific reaction zone. Adjustments were made to ensure the reaction occurred throughout the entire column but it leads to a 13% total annual cost (TAC) increase compared to the base case. In Case 2, optimization was applied to a system where reaction were distributed throughout the column without prior optimization, yielding a marginal 3.87% reduction in the TAC.

Keywords: Reactive-extractive distillation; Separation; Ternary azeotropic mixture; Resource conservation; Process Intensification

*Corresponding authors; E-mail addresses: savierk@sunway.edu.my; skzyang@outlook.com (Z. Kong); E-mail address: gsegovia@ugto.mx (J.G. Segovia Hernández).

1.0. Introduction

Over the past three years, the hybrid reactive-extractive distillation (RED) has emerged as an increasingly popular and innovative method for azeotropic mixture separation. Unlike traditional processes where the reaction and distillation steps are commonly carried out sequentially, RED integrates chemical reaction and physical separation into a single unit operation, akin to reactive distillation (RD). To enhance the separation of azeotropic mixtures, RED introduces an additional solvent through external injection that alters relative volatility, which makes it differ from the RD. A notable application of this approach was pioneered by Su et al. [1], employing a three-column RED (TCRED) to separate a tetrahydrofuran (THF), ethanol (Eth), and water ternary azeotropic mixture. In their TCRED system, the first column is a RD column that utilizes the hydration interaction between ethylene oxide (EO) and water, yielding ethylene glycol (EG) without the need for a catalyst, a highly advantageous feature in reactive-based distillation. The remaining azeotropic mixture containing THF and Eth is directed to the second and third columns of the extractive distillation (ED) process. Compared to the original pressure swing distillation (PSD) for the same separation mixture [2], they reported a remarkable reductions in the total annual cost (TAC) and carbon dioxide (CO_2) emission by about 60 to 80%.

Following the introduction of TCRED, the RED concept gained momentum, leading to the development of various RED configurations. One notable advancement is the double column reactive-extractive distillation (DCRED), which unites both RD and ED within a single column known as the reactive-extractive distillation column (REDC). In this configuration, the fresh feed, reactant, and solvent are introduced simultaneously, and the resulting EG serves as a solvent for facilitating the separation of azeotropic mixtures. Wang et al. [3] demonstrated the effectiveness of DCRED in separating a ternary azeotropic mixture comprising ethyl acetate (EA), Eth, and water. Their simulations revealed an additional 20% to 35% improvement in TAC and CO_2 emissions compared to TCRED. Notably, when comparing DCRED with conventional distillation processes like the triple column ED, the improvements are even more substantial, ranging from 50% to 100%. This demonstrates the considerable potential of RED configurations in advancing separation processes. As a result of the successful introduction of DCRED, several subsequent studies have also explored the application of DCRED for the separation of other ternary azeotropic mixture such as cyclohexane (CY)/isopropanol (IPA)/water [4], benzene/IPA/water [5], and IPA/EA/water [6].

In addition to TCRED and DCRED, several studies have explored other intensified RED systems, such as thermally coupled RED (TC-RED) [7], side-stream RED (SS-RED) [8], and dividing-wall RED (DWRED) [9], to further enhance the separation process performance of RED. These studies are comprehensively summarized in **Table 1**, which will be presented in **Section 2** to maintain the logical flow of this study. Moreover, for interested readers, detailed information regarding these various RED configurations can be found in our previous review [10,11]. Other than that, studies have also begun to explore the potential applications of RED in the production of various chemicals, such as isopropyl acetate [12], n-butyl acetate [13], and in transesterification reactions [14]. Such increasing popularity of RED research reflects its significance and effectiveness, and it is anticipated that more studies on RED will continue to emerge in the coming years.

Despite the various advantages reported in existing literature, it is essential to note that some research endeavors have also ventured into exploring potential side reactions within the RED system [15,16], driven by the objective of uncovering the drawbacks and limitations of the RED system. Apart from the inevitable side reactions, another significant gap in the existing

body of RED studies pertains to the optimization algorithm. As such, the primary focus of this work revolves around optimizing RED, where we aim to address several associated challenges, as detailed in **Section 2**. The remainder of this manuscript follows this structure: **Section 3** elaborates on the case studies and the methodology employed in this research. **Section 4** is dedicated to presenting and discussing the results. Lastly, **Section 5** provides recommendations for future work and concludes this study.

2.0. Problem statement

Table 1 shows the summary of studies done on RED for ternary azeotropic mixture containing information such as the components in mixture, optimization objective, and algorithm. Here, we aim to address and discuss two specific challenges.

1. From **Table 1**, one important observation made was that the majority of the existing studies have carried out process optimization based on minimum cost (i.e., TAC) as the objective function to obtain the optimal column configuration. There are various optimization algorithm being employed, i.e., genetic algorithm (GA), multi-objective genetic algorithm (MOGA), multi-objective particle swarm optimization (MOPSO), sequential iterative optimization (SIO), non-dominated sorting genetic algorithm-II (NSGA-II), and particle swarm optimization (PSO). The optimization variables generally include the solvent flow rate, total number of trays, feed locations, reflux ratios, reboiler duties, operating pressures, purge flow rate, liquid holdup, and reactive stages. However, it is important to remember that the hydration reaction of EO is an uncatalyzed reaction, and the reaction is expected to take place throughout the entire column [17]. Thus, it is not necessary to include the reactive stages as one of the optimization variables, but most of the existing studies have done so. Although there are two studies in **Table 1** that allow the reaction to take place throughout the column [4,17], it is important to highlight that no optimization was carried out in Ref. [17], and the authors set the reaction to take place throughout the entire column. In Ref. [4], the authors relied on a more simplified optimization algorithm due to the complexity of their process under study. In fact, the most appropriate way for process optimization in this case is to optimize only the total number of stages, and the reactive stage should generally follow the total number of stages, which is not the case in most of the existing studies. However, such optimization is difficult to carry out due to the variable overlap issue between MATLAB and Aspen Plus.
2. According to Zhang et al. [17], the holdup for the top (i.e., condenser) and last (i.e., reboiler) should be 10 times those of normal stages in the middle of the column. Therefore, three different holdup values need to be defined in Aspen Plus, and each holdup has its own starting and ending stage. For example, given that the total stages are 95, the starting and ending stage for the top holdup is generally 1 to 1, while the starting and ending stage of the bottom holdup (i.e., reboiler) should be 95 to 95. The starting and ending stage for the middle stages holdup is 2 to 95. Building a specific code that allows the reactive stages specification in Aspen Plus during the optimization process is a challenging task, especially considering the variable overlap issue. It is necessary to ensure that when the total number of stages changes, the ending stage of the middle stages and the bottom stages changes accordingly. It is speculated that

previous studies may have chosen to optimize the reactive and total stages separately and we believe that it is due to the challenges in building such a code.

In this study, our goal is to propose an optimization procedure tailored for the RED system. It is essential to clarify that our aim is not to definitively claim that the optimization method we develop here is the ultimate solution providing a global optimum. Instead, our contribution lies in optimizing the RED system in a more precise (i.e., "correct") manner. We achieve this by designing a specific algorithm capable of allowing the reactive stage to follow the total number of stages throughout the optimization process. This innovative approach eliminates the "variable overlap" problem, which is a departure from the commonly used methods in most existing studies. We believe that our proposed procedure has the potential to yield refined RED designs that closely mimic real-world conditions.

Table 1. Summary of studies on RED for ternary azeotropic mixture

No.	System	Algorithm	Objective	Include reactive stage as variable?	Reaction zone	Ref.
1	EA/Eth/Water	GA	Cost	✔	Partial	[3]
2	THF/Eth/Water	MOGA	Cost	✔	Partial	[1]
3	Tert-butyl alcohol(TBA)/Eth/Water	-	Cost	-	Whole column	[17]
4	THF/Eth/Water	-		-		
5	Acetonitrile(ACN)/IPA/Water	-		-		
6	TBA/Eth/Water	MOPSO	Cost	✔	Partial	[18]
7	ACN/IPA/Water	SIO	Cost	✔	Partial	[19]
8	EA/Eth/Water	MOGA and NSGA-II	Cost, environment, and safety	✔	Partial	[9]
9	IPA/Diisopropyl ether(DIPE)/Water	PSO	Cost	✔	Partial	[20]
10	THF/Eth/Water	PSO	Cost	✔	Partial	[21]
11	Benzene/IPA/Water	MOGA NSGA II	Cost, environment, and thermodynamic efficiency	✔	Partial	[5]
12	IPA/EA/Water	PSO	Cost	✔	Partial	[8]
13	CY/IPA/Water	SIO	Cost	-	Whole column	[4]
14	TBA/Eth/Water	SIO	Cost, environment, and thermodynamic efficiency	✔	Partial	[22]
15	IPA/EA/Water	PSO	Cost	✔	Partial	[6]
16	ACN/IPA/Water	NSGA-II	Cost	✔	Partial	[23]

2.0. Methodology

The methodology employed in this study is illustrated in **Figure 1**. Initially, we chose two distinct DCRED configurations from previous research studies [3,17]. These configurations served as our base cases for subsequent comparisons. Next, we applied our newly developed optimization procedure to optimize the two case studies. Finally, we compared the optimized configurations to the base cases, evaluating them based on energy and economic indicators.

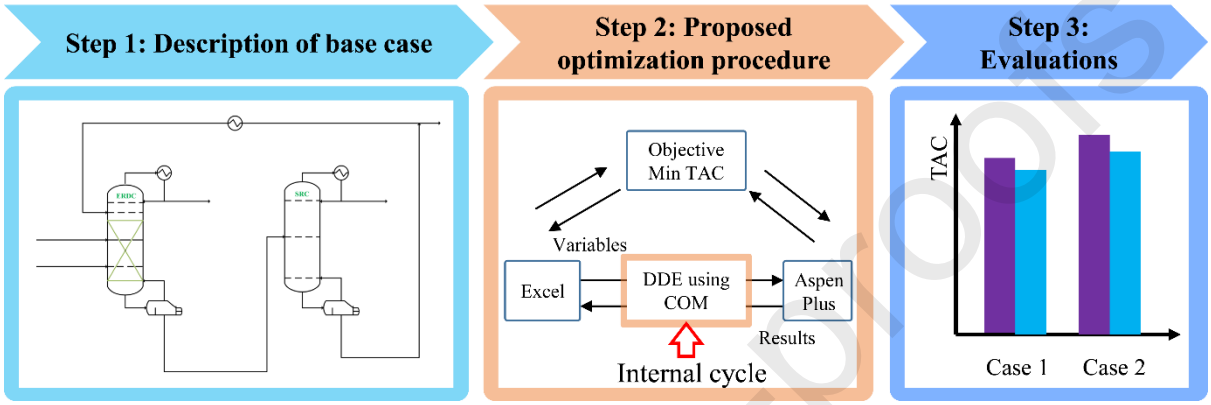

Figure 1. An overview of the methodology utilized in this study.

2.1. Description of base case

2.1.1. Case 1

Figure 2 depicts the reproduced DCRED process for the ternary azeotropic separation of EA, Eth, and water. This case study was chosen because it is one of the earliest work that demonstrated the use of DCRED. Note that in this case, the designated reaction zone spans from stage 11 to stage 41, as depicted in **Figure 2**. Our specific objective in this case is to examine the impact of appropriately configuring and optimizing the reaction to occur throughout the entire column. We aim to determine whether this adjustment leads to performance enhancements or introduces any potential adverse effects to the process. In **Figure 2**, a 100 kmol hr^{-1} fresh feed containing 30 mol.% of EA, 20 mol.% of Eth, and 50 mol.% of water is fed into the REDC. To enable the necessary hydration of EO as per **Eq. 1**, it is necessary to introduce an equal amount of EO compared to the water in the fresh feed, which amounts to 50 kmol hr^{-1}. A large amount of EG (225 kmol hr^{-1}) is also added to the REDC to boost azeotropic separation. The distillate from the REDC should achieve a recovered EA purity of 99.64 mol.%. The remaining mixture of Eth and EG is directed to the solvent regeneration column (SRC), where recovered Eth with a purity level of 99.66 mol% is obtained as the distillate, and recovered EG with a purity level of 99.92 mol% is collected as the bottom product. Before being recirculated into the REDC, the regenerated EG undergoes a cooling process. Any surplus solvent within the system is removed through a purging mechanism.

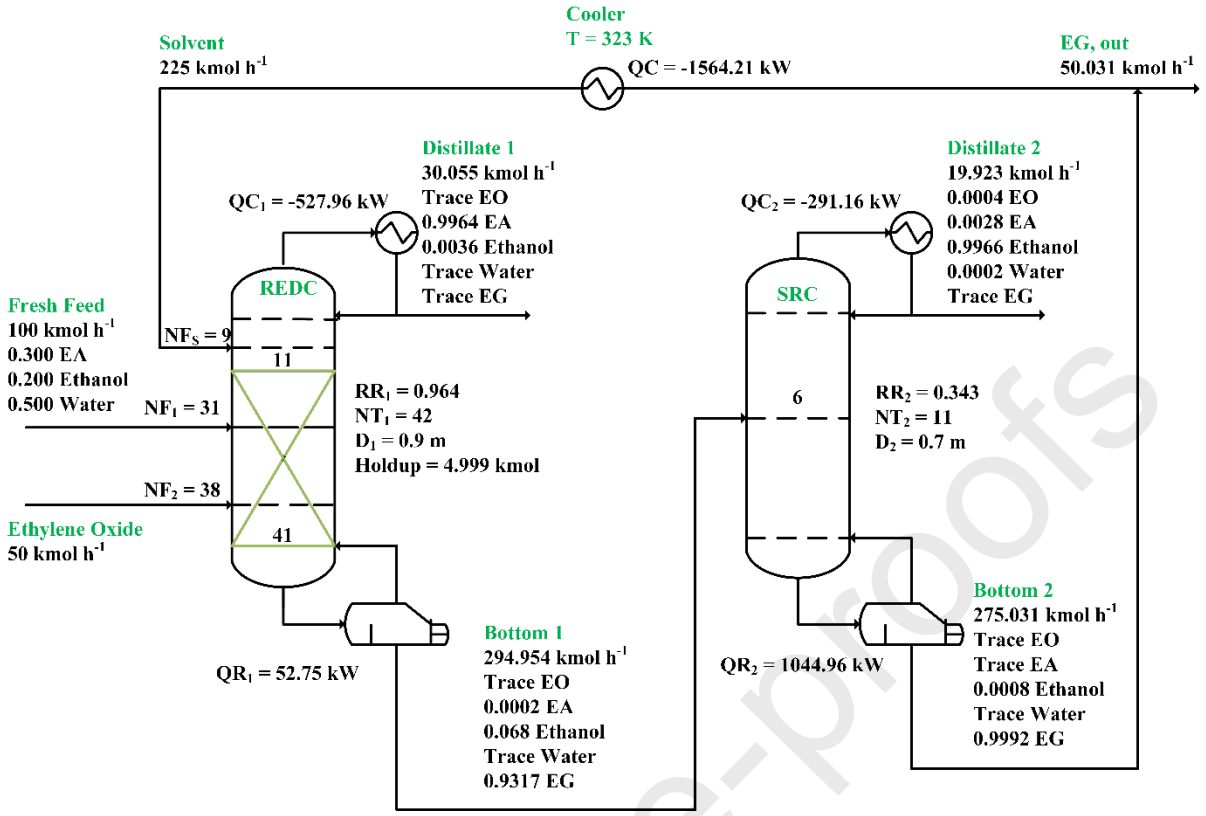

Figure 2. Flowsheet of DCRED for ternary azeotropic separation of EA/Eth/water reproduced from Ref. [3].

$$EO + Water \rightarrow EG \qquad \textbf{(Eq. 1)}$$

$$r_1\left(\frac{mol}{s^* cm^3}\right) = 3.15 \times 10^9 exp\left(\frac{-9547}{T}\right) x_{water} x_{EO}$$

2.1.2. Case 2

The second case study was adopted from Ref. [17] for the ternary azeotropic separation of ACN, IPA, and water. The reason behind selecting this case study was twofold. Firstly, the original process developed by Ref. [17] already allowed for reactions to occur throughout the column, but it had not been optimized. Thus, we aimed to investigate the impact of optimization and assess if performance improvements were attainable. Secondly, this case study also represents one of the earliest instances where RED was employed for the separation of a ternary azeotropic mixture. The reproduced flowsheet is depicted in **Figure 3**. In this process, the REDC initially receives a fresh feed stream of 100 kmol hr^{-1}, consisting of 30 mol. % ACN, 30 mol. % IPA, and 40 mol. % water. Identical to Case 1, it is necessary to provide an amount of EO (i.e., 40 kmol hr^{-1}) equivalent to that of water in the fresh feed to facilitate the EO hydration (**Eq. 1**). This balanced introduction ensures the complete elimination of water while generating sufficient EG to serve as a solvent for subsequent azeotropic separation within the same column.

To enhance the EG solvent quantity for effective azeotropic separation, an additional 90 kmol hr^{-1} of EG is introduced into the REDC. The objective for the REDC is to produce a distillate stream with a recovered ACN purity of 99.9 mol.%. The remaining mixture, comprising IPA and EG solvent, is directed to the SRC. Within the SRC, a distillate stream is obtained, containing recovered IPA at a purity of 99.9 mol.%, while the bottom product consists of EG with a purity of 99.94 mol.%. Prior to recycling back to the REDC, the regenerated EG undergoes a cooling and purging process, identical to Case 1.

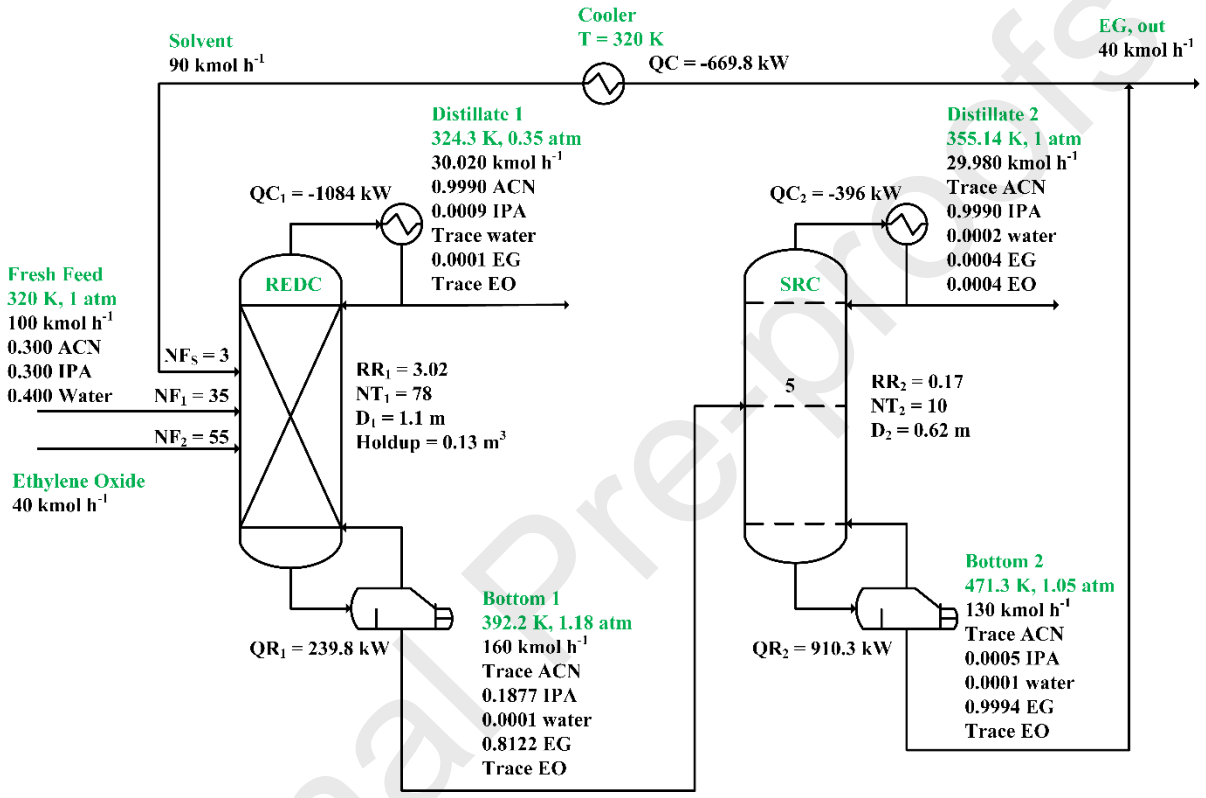

Figure 3. Flowsheet of DCRED for ternary azeotropic separation of ACN/IPA/water reproduced from Ref. [17].

2.2. Proposed optimization procedure

Efficiently operating any industrial processes is crucial for maintaining competitiveness in the current process landscape, especially when dealing with low productivity. To address this, the optimization problem is defined for each process sequence, taking into account the specific goals, limitations, and design parameters involved. As a result, all design challenges are framed as an optimization stochastic problem with constraints.

In each case study, the primary goal is to minimize the TAC, which directly correlates with the heat duty, services, and column size. Achieving this objective is contingent upon meeting the necessary recoveries and purities in each product stream, that is to say:

$$\min(TAC) = f\ (N_{tn}, N_{fn}, R_{rn}, F_{rn}, D_{cn}, H_{un}) \quad \textbf{(Eq. 2)}$$

$$subject\ to\ \overrightarrow{y_m} \geq \overrightarrow{x_m}$$

The optimization involves various parameters within the process. These include N_{tn} as the total column stages, N_{fn} representing feed stages in columns, R_{rn} denoting the reflux ratio, F_{rn} signifying distillate fluxes, D_{cn} for column diameter, H_{un} as hold up, and y_m and x_m representing vectors for obtained and required component purities, respectively. Minimizing these parameters necessitates the manipulation of 15 continuous and discrete variables for each process route. It is crucial to note that, due to product stream flows being influenced by chemical reactions, the purities of key components in these streams must be accounted for as constraints in the optimization problem. The optimization and design of process routes are intricate, non-linear, and multivariable challenges, featuring both continuous and discrete design variables [24,25]. Moreover, the objective functions used in the optimization criteria can be nonconvex, potentially leading to the presence of local optima while adhering to certain constraints.

To address these complexities and optimize the process routes, we employed a stochastic optimization technique known as Differential Evolution with Tabu List (DETL). This is since stochastic optimization methods usually do not necessitate a precise starting point in the search. Unlike deterministic optimization techniques, which heavily depend on the initial guess to direct the search, stochastic optimization methods employ randomness to explore the search space more extensively. In particular, DETL method is designed to explore the search space more extensively, rather than being confined to a specific starting point. They employ mechanisms such as mutation, crossover, to explore different regions of the search space, even without a particularly good initial guess. The randomization inherent in this method allow to escape local optima and continue exploring the search space for better solutions. This method typically relies on convergence criteria based on the behavior of the objective function or the optimization process itself, rather than being heavily influenced by the initial guess. Other than that, stochastic optimization methods can work with black box or grey box models. In the particular case of this case study, this advantage allows not having to explicitly code the model to represent the process schemes. Thus, the Aspen Plus simulator is used so that the process model can be solved laterally. This implies that during the optimization process, multiple evaluations are performed on the process scheme that is modeled with all the complexity previously mentioned. Nonetheless, a consequence is that the computation times may increase significantly due to the multiple evaluations performed on the complex process scheme [26,27]. This prolonged convergence time is a direct result of the detailed evaluation of the complex system. Other drawbacks of DETL include the fact that the performance of DETL can be sensitive to parameter choices, including population size, crossover probability, and mutation factor. Fine-tuning these parameters for optimal performance can be time-consuming and computationally intensive.

As a historical note, Differential Evolution (DE) draws inspiration from Darwin's natural selection theory, resembling GA with a significant difference, i.e., DE encodes decision variables as floating-point numbers, not bit strings. Srinivas and Rangaiah [28] demonstrated that integrating tabu search concepts could enhance the DE algorithm's performance. Notably, the tabu list (TL) is utilized to prevent revisiting already explored regions in the search space,

thus minimizing unnecessary function evaluations. Building on this concept, Srinivas and Rangaiah [28] introduced the hybrid approach DETL, which combines traditional DE steps with TL and tabu checks to monitor evaluated points and avoid revisits during optimization. A convergence criterion based on the maximum number of generations is also implemented. A detailed description of the DETL algorithm is available in Ref. [28].

The implementation of this optimization approach involves a hybrid platform using Microsoft Excel and Aspen Plus. Decision variable vectors are transmitted from Microsoft Excel to Aspen Plus through Dynamic Data Exchange (DDE) *via* component object model (COM) technology. Particularly, COM is a fundamental technology in Microsoft Windows for software development. It enables interprocess communication and code reuse through a component-based architecture. Key aspects of COM include its language-agnostic nature, interface-based communication, object activation, lifetime management, and support for versioning and backward compatibility. In Microsoft Excel, these values are assigned to the process variables required by Aspen Plus. After simulation, Aspen Plus sends back the resulting vector to Microsoft Excel, where the objective function values are analyzed, and new decision variable values are proposed based on the chosen stochastic optimization method.

During the optimization process, the algorithm assigns a vector to all design variables, necessitating the generation of appropriate physical constraints within inner cycles. For instance, when the algorithm proposes a total stage count X and a feed stage Y, Y must logically be less than X for physical coherence. However, the algorithm may not inherently recognize the clear physical meanings of these variables, potentially leading to scenarios where Y exceeds X. Therefore, the coding of variable assignment must include necessary constraints associated with internal cycles and the variables proposed by the optimization algorithm to ensure proper physical significance and direct impact on the objective function and input-output readings. Throughout the optimization stage, an iterative process evaluates the process model using vectors containing the process design variables, resulting in the attainment of the objective function's value associated with the optimized model. The coding methodology discriminates between vectors satisfying certain optimization problem constraints, typically linked to mass and energy balance, as well as product purities. Constraints related to process scheme topology, such as ensuring the feed stage value is less than the total stage count, can be established. Similarly, constraints can be coded to align the start and end of the reactive zone with specific column stages. Failure to meet these constraints results in the optimization method recognizing the variable vectors as unsuitable for the coded optimization problem.

To express the internal constraints associated with the process design within the coding of the optimization algorithm, especially when the value of one design variable depends on another in an internal cycle, one can mathematically describe this as follows:

1. Let us denote the vector of decision variables as *x*, which includes design variables and associated parameters. The optimization algorithm aims to minimize or maximize a set of objective functions *f(x)* based on these decision variables. The internal constraints are represented as equations that establish relationships among the decision variables. Specifically, when one design variable x_i influences another design variable x_j, an internal constraint is formed. This can be mathematically expressed as:

$x_j = g(x_i)$ **(Eq. 3)**

where x_i is one of the design variables whose value is determined by the optimization algorithm, x_j is another design variable whose value is dependent on x_i, and $g(x_i)$ is a function that relates the value of x_i to the value of x_j. Thus, the optimization algorithm assigns values to the design variables, which include x_i. This assignment is done iteratively as part of the optimization process.

2. Within the optimization algorithm, there exists an internal loop or iterative process that adjusts the values of the design variables, including x_i and subsequently x_j. This loop continues until convergence is achieved, ensuring that the internal constraint, represented by the **Eq. 3** is satisfied.
3. The internal loop within the optimization algorithm operates iteratively, adjusting the values of x_i and, consequently, recalculating the value of x_j using the relationship defined by the function $g(x_i)$. The internal loop continues until a predefined convergence criterion is met, indicating that the internal constraints are satisfied, and the values of the design variables, including x_i and x_j, have reached optimal or acceptable values.

The above mathematical description outlines the process of incorporating internal constraints associated with the process design within the optimization algorithm's coding. It emphasizes the dependencies between design variables and the need for an iterative process to ensure these internal constraints are met during the optimization process. In this way, it is possible to rectify and indirectly reassign values of design variables using some previously proposed by the optimization algorithm, and that these variables have a direct impact on the value of the objective function so that they have an impact on the generation of a new population of vectors for the next generation to be evaluated. This consideration can be applied in the assignment of values for the feeding stage, the specification of the start and end of the reactive column section, and that this is in accordance to the stages with an adequate holdup value, etc. By doing so, our optimization focuses on the total number of stages while ensuring that the reactive stage corresponds to this total, a deviation from many existing studies. These internal constraints play a pivotal role in mitigating the "variable overlap" issue, a deviation from the prevalent methods in current research. We are confident that our proposed procedure holds the potential to yield optimized RED designs that closely emulate real-world conditions. The overall optimization framework is graphically illustrated in **Figure 4**.

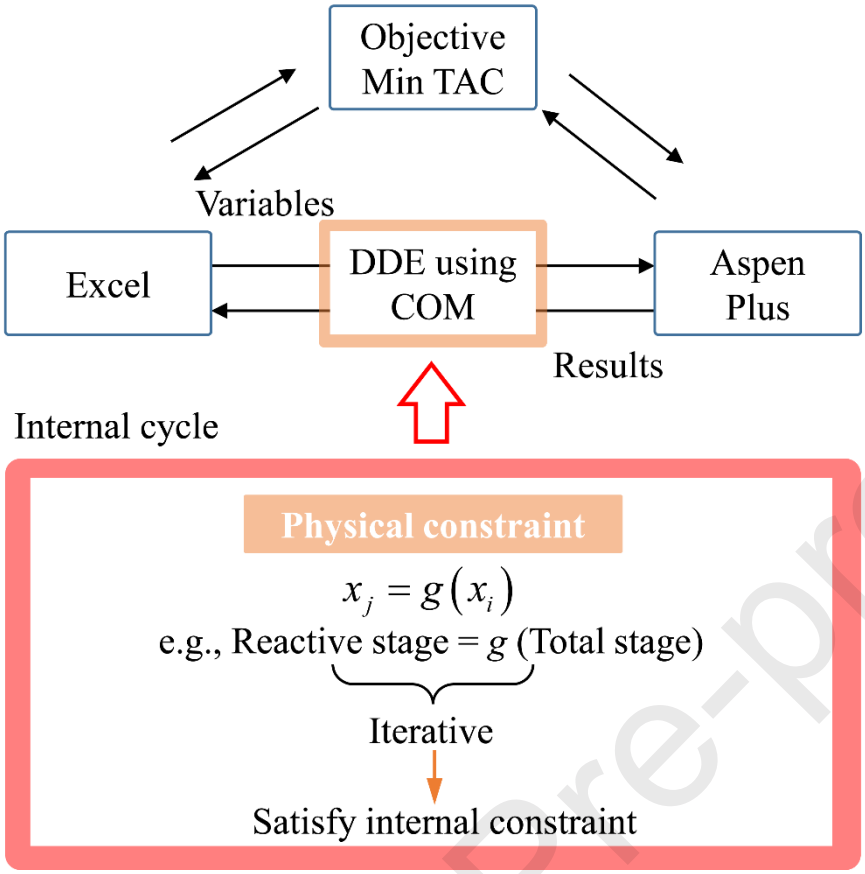

Figure 4. Graphical representation of the overall optimization framework.

For the specific process routes analyzed in this study, we utilized the following parameters for the DETL method: 200 individuals, 300 generations, a tabu list comprising 50% of the total individuals, a tabu radius of 0.0000025, and crossover and mutation fractions set at 0.80 and 0.6, respectively. These parameter settings were determined through a tuning process involving preliminary calculations, where different combinations of individuals and generations were tested to identify the optimal parameters that would yield the best convergence performance for DETL. These parameters are also identical to those recommended by Srinivas and Rangaiah [29], which have been successfully tested in several case studies with a similar complexity [30,31].

To calculate the TAC, which serves as the objective function, we employed the method originally developed by Guthrie (1969) and later modified by Ulrich (1984). This method estimates the cost of an industrial plant by segmenting it into various units, utilizing equations provided by Turton et al. (2008) for an approximate cost assessment of the process using **Eq. 4**, as follows:

$$TAC = \frac{\sum_{i=1}^{n} C_{TM,i}}{n} + \sum_{j=1}^{n} C_{ut,j} \quad \textbf{(Eq. 4)}$$

In this context, TAC represents the comprehensive yearly expenses, C_{TM} stands for the initial capital expenditure of the facility, n corresponds to the period required for financial return, and C_{ut} designates the expenditure linked to services.

3.0. Results and discussion

3.1. Case 1

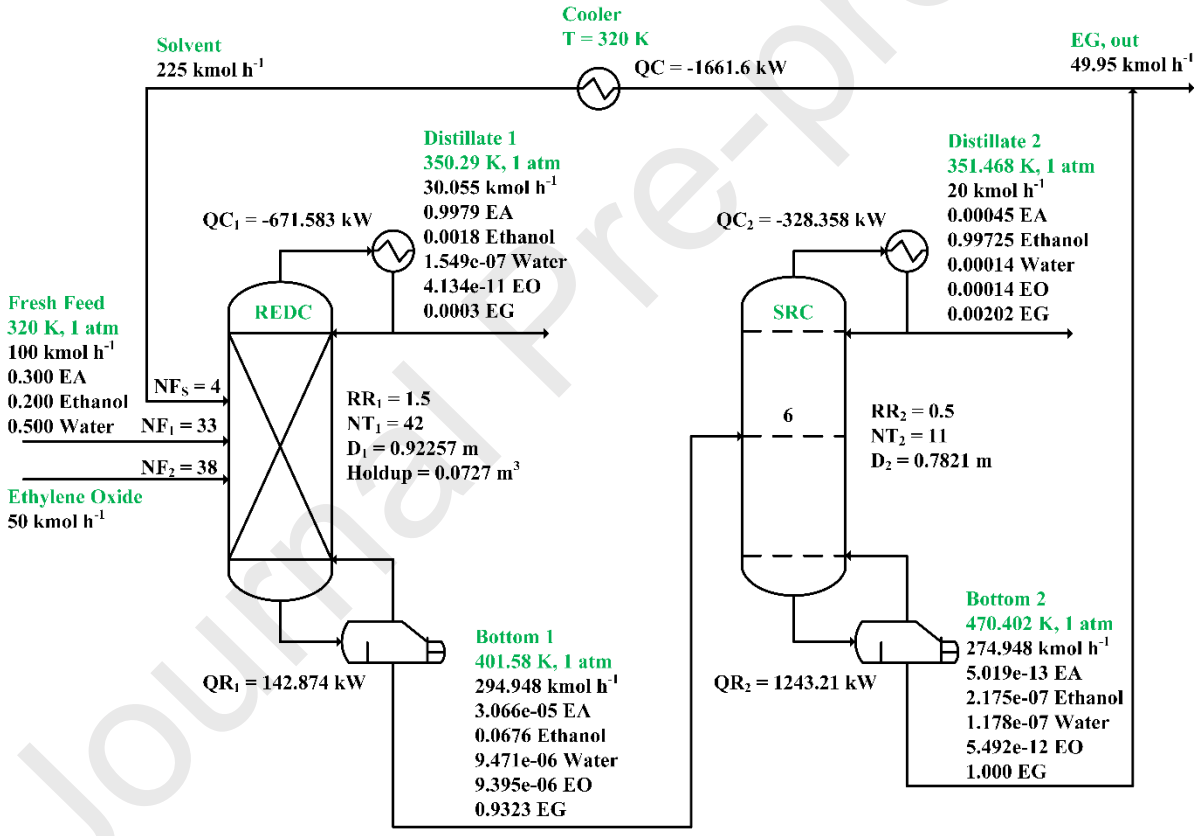

Figure 5. Modified flowsheet for Case 1.

Figure 5 presents the modified base case for Case 1. Here, we have adjusted the flowsheet so that the reaction occurs throughout the entire column, as opposed to being limited to specific sections as in the original base case (**Figure 2**). It is important to emphasize that we made this modification to facilitate the use of this case as an initial configuration for the subsequent optimization process. Alongside enabling the reaction throughout the column, another significant alteration involved the liquid holdup. We must acknowledge that we are uncertain

about how the liquid holdup was calculated in the base case [3] as the specific details, to our knowledge, were not provided. In the original base case, the holdup was reported in terms of kmol, whereas the convention we commonly encounter is reporting it in m^3. We want to clarify that we are not implying any error in their approach, as we understand that Aspen Plus can represent holdup in kmol as well. Our intention is simply to share that the more common reporting convention we have encountered is usually in m^3. Additionally, we noticed that previous authors expressed gratitude to a reviewer for suggesting the holdup calculation, yet the formula was not provided in the literature. Consequently, we decided to adjust the liquid holdup using the formula suggested by Ref. [17], which reports it in m^3.

Following these two significant modifications (i.e., extending the reaction zone and modifying the holdup volume), it became necessary to make adjustments to the column configuration to achieve the desired product purities. Firstly, the total number of stages in the REDC remain unchanged (42 stages). We relocated the fresh feed location, increasing it in the modified case to the 33^{th} stage, in contrast to the 31^{st} stage in the original base case. The EO feed stage was remained at 38^{th} stage, and the solvent inlet location was moved upwards from the 9^{th} stage to the 4^{th} stage. These alterations in the column topology resulted in an increase in reboiler duty in REDC by approximately 170.85%. In the case of the SRC, the total number of stages and feed location were kept constant at 11 stages and 6^{th} stage. These changes in column configuration led to an increase in the SRC reboiler duty by approximately 18.97%, rising from 1044.96kW to 1243.21kW. Altogether, these modifications translate to an increase in TAC by about 16% from \$0.917 to \$1.066 million. Subsequently, the modified base case (**Figure 5**) will undergo process optimization using our proposed procedure to determine the optimal column configuration and further reduce the TAC.

Figure 6 illustrates the results obtained from optimizing Case 1, and the optimized process configuration is shown in **Figure 7**. This optimization process spanned approximately 4 days, with the TAC stabilizing at around \$1.033 million after roughly 20,000 iterations. In terms of total energy consumption, the optimized configuration delivers 1304.55kW. These outcomes signify an 3.1% decrease in TAC and an 5.88% decrease in total energy consumption when compared to the modified base case (**Figure 5**).

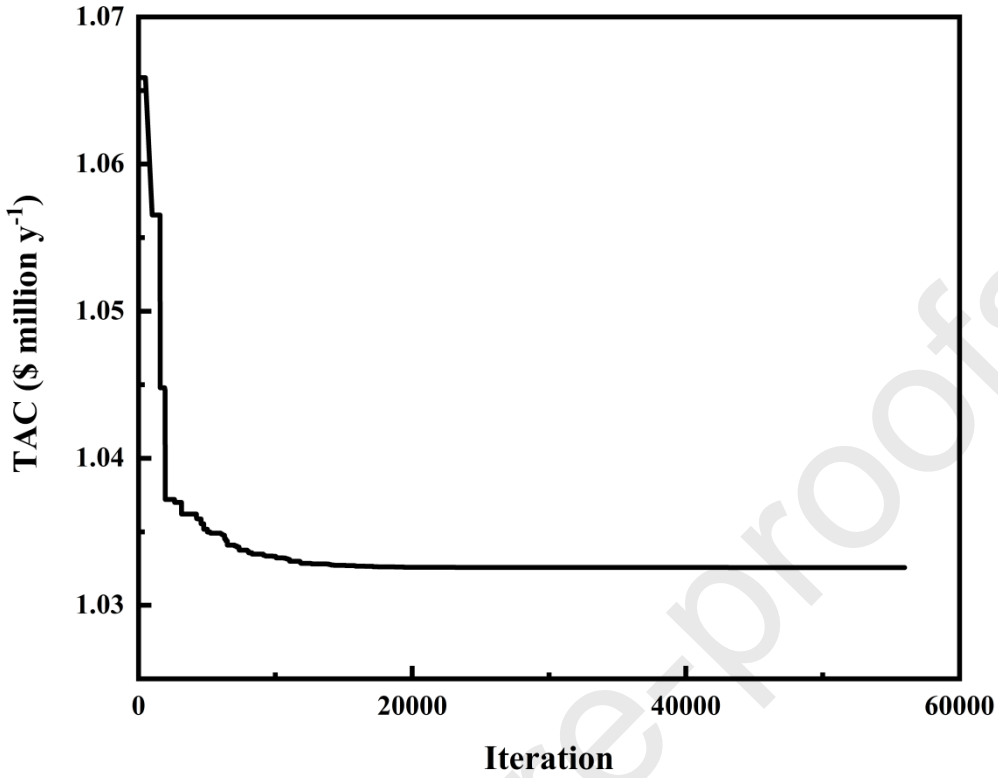

Figure 6. Optimization result for Case 1.

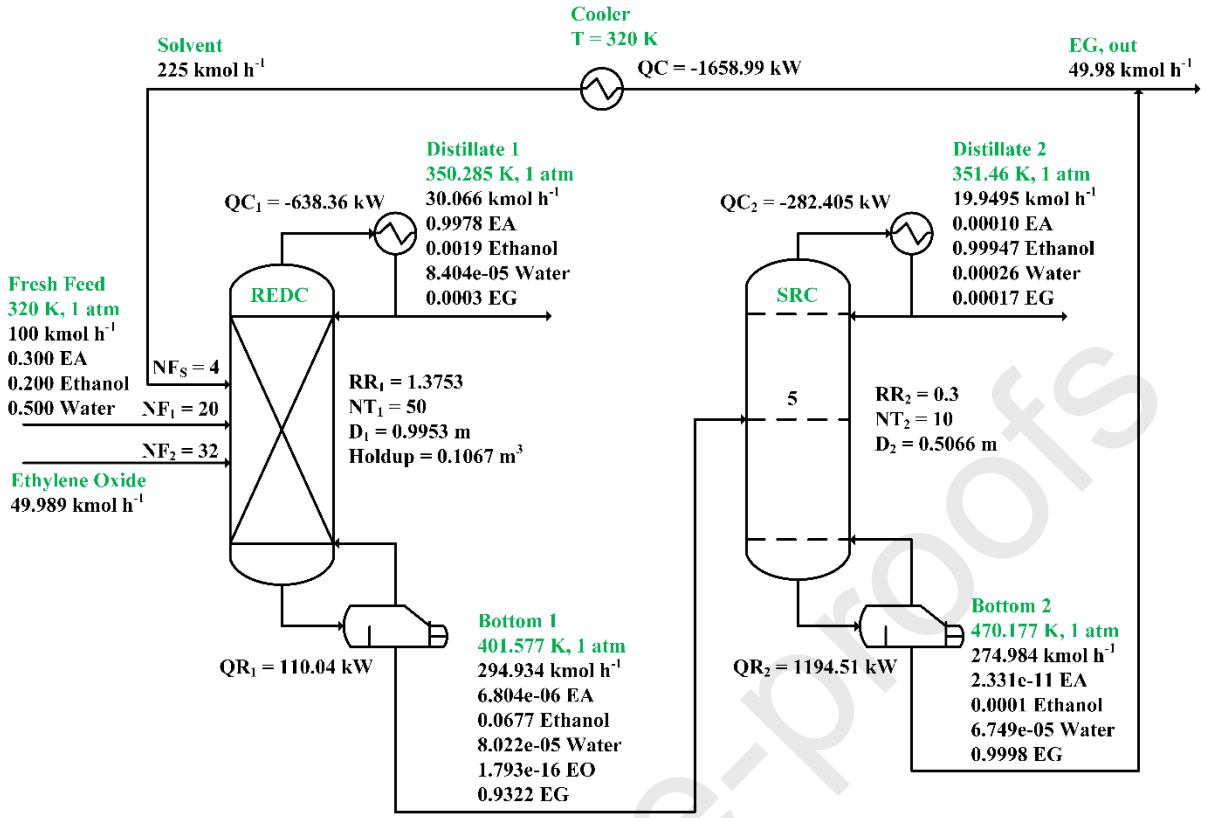

Figure 7. Optimized flowsheet for Case 1.

In terms of column configuration, a thorough comparison unveiled that the optimized REDC demanded higher stages, specifically 50 stages (**Figure 7**), as opposed to the 42 stages required in the modified base case (**Figure 5**). This reduction translated into a substantial increase in total capital cost (TCC). Notably, the optimized REDC positioned its fresh feed stage higher, specifically at the 20th stage, whereas the modified base case had it at the 33rd stage. A similar trend was observed for the reactant feed stage, with the optimized REDC locating it at a higher stage (32nd stage) compared to the modified base case at the 38th stage. Concerning the solvent feed location, it was remained from at the 4th stage after optimization. Regarding reboiler duty, the optimized REDC exhibited a substantial increase of 22.98%, decreasing from 142.874kW in the modified base case (**Figure 5**) to 110.04kW (**Figure 7**). This reduction significantly contributed to the overall decrease in total operating cost (TOC). Note that both the optimized and base cases maintained nearly the same reboiler temperature range (i.e., below 433K). Consequently, both configurations utilized the same grade of heating utility, and this factor did not contribute to the reduction in TOC. This contrasts with some existing studies where variations in steam grade played a significant role in TOC reduction [35,36].

As for the SRC, it was observed that the optimized configuration required fewer total stage, totaling 10 stages, compared to the modified base case with 11 stages. Additionally, the optimized SRC featured a smaller diameter, approximately 35.23% smaller at 0.5066m, compared to the modified base case at 0.7821m. Both the decrease in the total number of stages and column diameter resulted in an decrease in the TCC. Concerning the feed location, it was positioned higher, specifically at the 5th stage, in contrast to the modified base case where it was at the 6th stage. Lastly, regarding reboiler duty, there was a significant decrease of 3.92%,

rising from 1243.21kW in the modified base case to 1194.51kW in the optimized configuration. We believe that this decrease had contributed significantly to the reduction in TOC.

Here, it is interesting to also compare the column configuration between the optimized case (**Figure 7**) against the original base case (**Figure 2**) as they exhibit distinct features in terms of the reaction zone and how the holdup was computed. Upon a detailed comparison between **Figure 7** and **Figure 2**, it was observed that the REDC in the optimized scenario required a higher number of stages, specifically 50 stages in **Figure 7**, compared to the 42 stages in the original configuration (**Figure 2**). Notably, the fresh feed stage of the REDC occurred in the 31st stage before optimization, whereas after optimization, it moved up to the 20th stage. Furthermore, in the original base case scenario, EO was introduced into the REDC at the 38th stage, while after optimization, EO was introduced at the 32nd stage. The recycled solvent, before optimization, entered the system at stage 9, whereas after optimization, it entered at stage 4. In terms of the reboiler duty, it is noteworthy that the optimized REDC necessitates almost twice the duty compared to the original base case. Since both configurations utilized the same grade of heating utility, the contribution to the TOC stemming from the reboiler duty remained virtually unchanged between the optimized case (**Figure 7**) and the original base case (**Figure 2**). In terms of the SRC column configuration, the optimization results revealed several noteworthy changes. The optimized SRC, in particular, required one less number of stages, totaling 10 stages, compared to the original base case with 11 stages. As for the feed stage entering SRC, the original base case placed the feed stage at the 6th stage while in the optimized case, the feed location to SRT shifted one stage upward to the 5th stage. The SRC reboiler duty experienced a substantial increase of 14.3%, rising from 1044.96kW to 1194.51kW.

Overall, we illustrated here a scenario where the original base case featured a confined reaction limited to a specific zone rather than spanning the entire column. Additionally, the method used for calculating the holdup differed slightly from common practices outlined in existing literature. Therefore, certain modifications were necessary to ensure that the reaction was accurately occurring throughout the entire column, aligning with the nature of an uncatalyzed reaction. We believe that such simulations better reflect real-world scenarios. Due to these modifications, the TAC of the optimized case has increased by approximately 13% to \$1.033 million (**Figure 7**), compared to the original case at \$0.917 million (**Figure 2**). It may seem perplexing to observe an increase in TAC after optimization compared to the original base case. This discrepancy arises because the original configuration (**Figure 2**) was limited to a specific zone, necessitating modifications to enable reactions throughout the entire column. Consequently, after this modification (**Figure 4**), the TAC deviates from the original case at \$0.917 million. This divergence is expected since the modified case (**Figure 4**) undergoes a topological change in column configuration, differing from the base case (**Figure 2**).

Another possible question that may arise is whether the improvement (if any) is because of the incorporation of all stages as reactive stages or solely because of the use of a (better) optimization techniques. This is since the original case (**Figure 2**) was optimized using a genetic algorithm, whereas we employed the DETL algorithm for optimization in this work. Firstly, our perspective is that optimization does not necessarily guarantee enhancement, as we demonstrated here in Case 1. Hence, comparing scenarios before and after optimization becomes challenging due to the inherent differences resulting from model modifications aimed at enhancing simulation realism. One should also remember that our objective is not solely focused on achieving superior outcomes but rather on proposing a more accurate optimization approach reflecting real-world scenarios. Secondly, out of curiosity, we attempted to optimize

the original Case 1 (**Figure 2**) using DETL, with the corresponding flowsheet provided in the Supporting Information (**Figure S1**). It was found that the calculated TAC was slightly lower than that of the original Case 1 (**Figure 2**), by just under 1%. This marginal improvement is expected, considering the original Case 1 has already been optimized using a genetic algorithm. Therefore, there appears to be limited room for further improvement, even with another alternative optimization algorithm. Comparing the optimized case with reactions spanning throughout the entire column (**Figure 7**) and the optimized case with reactions confined to a specific section (**Figure S1**), it is evident that the former yields a significantly higher TAC. This again reflects the distinct nature of **Figure 2** (or **Figure S1**) and **Figure 7**, precluding a fair comparison between them. Importantly, this also suggests that the choice of optimization algorithm plays a minimal role in our study, at least from our perspective and findings.

In the next case, we will explore into another intriguing scenario where the reaction was initially configured to occur throughout the column but has not yet been optimize. Unlike Case 1, where modifications were needed to configure the reaction, Case 2 requires no such adjustments. Our objective here is to scrutinize the impact of optimization and evaluate whether it can yield performance improvements.

3.2. Case 2

Figure 8 presents the outcomes of the optimization process for Case 2, while the optimized process configuration is depicted in **Figure 9**. Here, it is worth noting that the reproduced base case shown in **Figure 3** can serve as the initial case without any alterations because the original setup already allowed the reaction to occur throughout the column. The optimization process took about 4 days, with the TAC stabilizing at about $ 0.944 million after approximately 30,000 iterations. As for the total energy consumption, the optimized configuration operates at 1061 kW. These results indicate a notable 3.87% reduction in TAC and a substantial 7.71% decrease in total energy consumption when compared to the replicated base case (**Figure 3**).

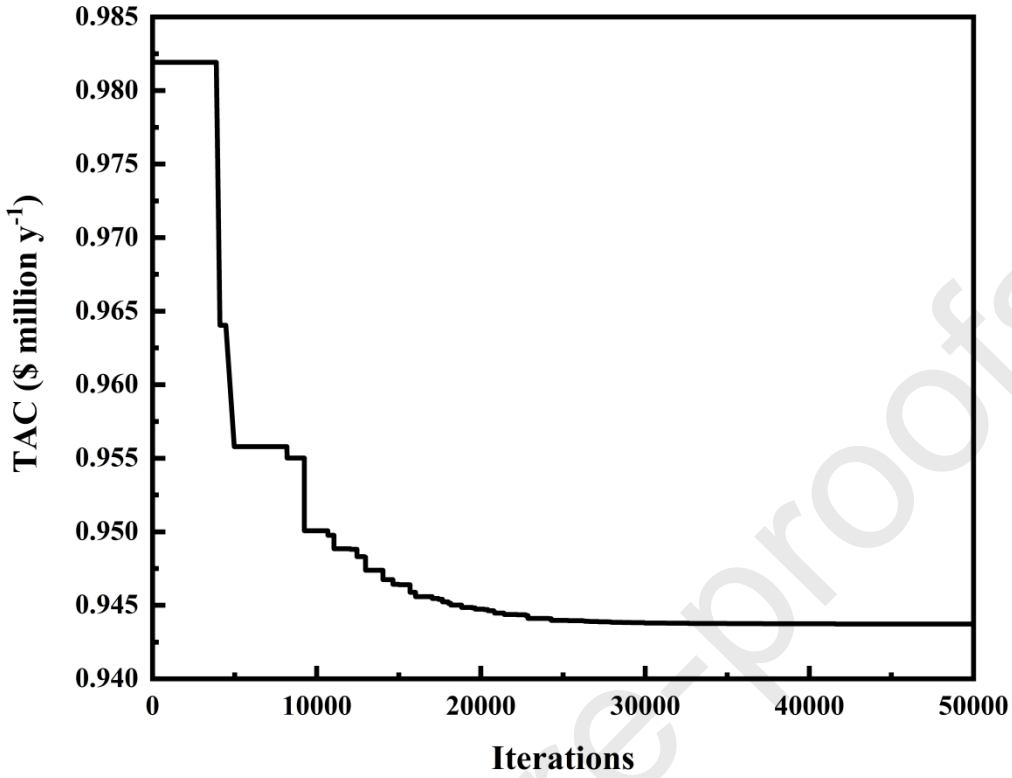

Figure 8. Optimization result for Case 2.

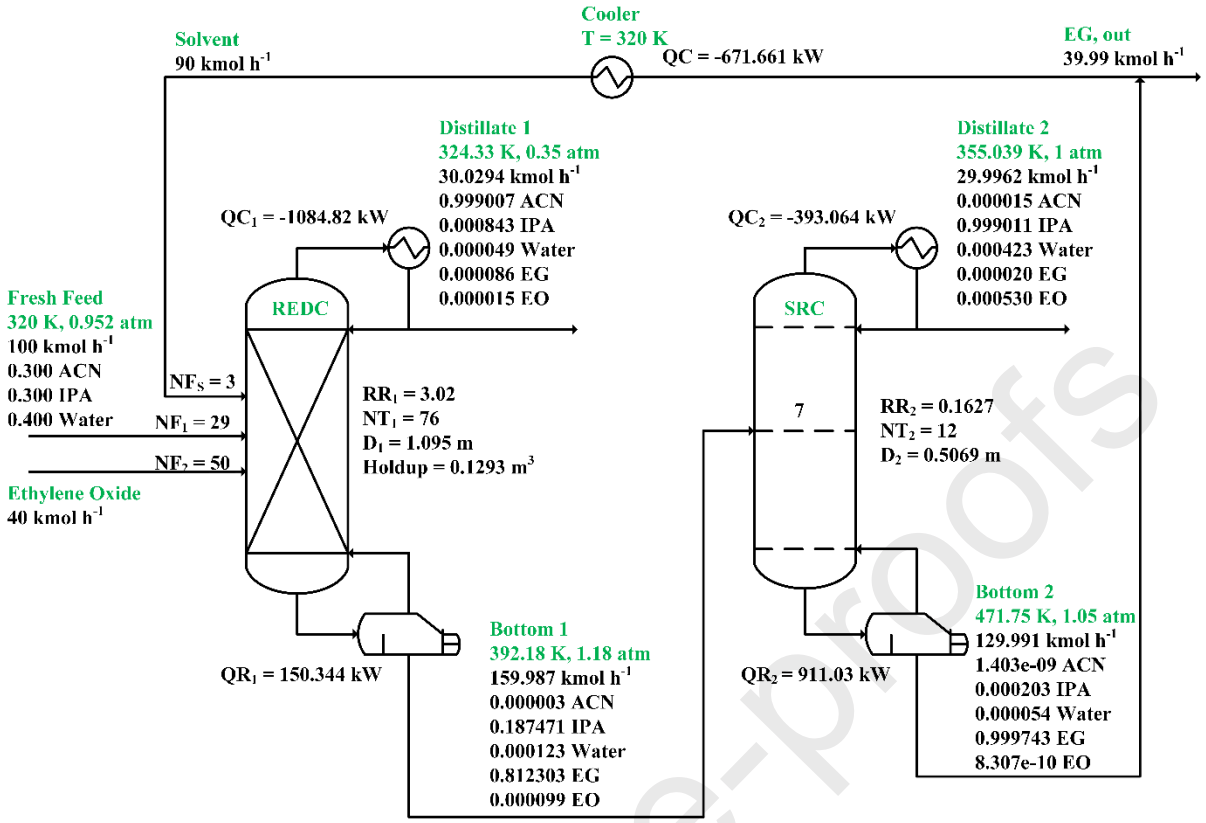

Figure 9. Optimized flowsheet for Case 2.

Regarding column configuration, a meticulous comparison revealed that the optimized REDC required fewer stages, specifically 76 stages (**Figure 9**), in contrast to the 78 stages in the base case (**Figure 3**). This reduction resulted in a marginal decrease in the TCC. Notably, the optimized REDC positioned its fresh feed stage higher at the 29th stage, while the base case had it at the 35th stage. A similar trend was observed for the reactant feed stage, with the optimized REDC locating it at a higher stage (50th stage) relative to the base case at 55th stage. Regarding reboiler duty, the optimized REDC (**Figure 9**) exhibited a significant reduction of 37.3%, decreasing from 239.8kW in the base case (**Figure 3**) to 150.344kW. This reduction translated to a lower TOC. It is noteworthy that, similar to Case 1, both the optimized and modified base cases maintained nearly the same reboiler temperature range (i.e., below 433K). Consequently, both configurations utilized the same grade of heating utility, and this factor did not contribute to the reduction in TOC.

For the SRC, it was noted that the optimized configuration required two more total stages, totaling 12 stages, compared to the base case with 10 stages. However, the optimized SRC featured a smaller diameter, approximately 18% smaller at 0.5069m, compared to the base case at 0.62m. This suggests a potential trade-off between the reduction in TCC due to the smaller diameter and the increase in TCC due to the addition of two extra stages. In terms of feed location, an opposite trend to that observed in the REDC became evident in the SRC. In the optimized configuration, the feed location was shifted downwards, precisely to the 7th stage, while the base case had it positioned at the 5th stage. Lastly, regarding reboiler duty, there was only a marginal increase of less than 0.1%, rising from 910.3kW in the base case to 911.03kW in the optimized configuration. We believe that this slight increase had an insignificant impact

on the overall TOC rise. The reboiler temperature remained identical in both the optimized and base cases, resulting in no variations in the heating utility grade, mirroring the observations made in the REDC.

Altogether, our simulations suggest that the decrease in reboiler energy consumption in the REDC and the decrease in the total number of stages in the REDC contributed to the overall reduction in the TAC. This is since there is not much reduction seen in the reboiler energy consumption of the SRC and as mentioned earlier, there may be a potential trade-off between the reduction in TCC due to the smaller diameter and the increase in TCC due to the addition of two extra stages. Hence, we believe that the changes in TCC and TOC in the SRC do not play a significant role in the overall reduction in TAC. We understand that the 3.87% reduction in TAC may appear minimal, and its contribution seems limited compared to the base case. However, we would like to emphasize that the optimized configuration presented in **Figure 9** represents a more precise and realistic approach closely mimicking real-world conditions. The optimization algorithm we developed here allows the reactive stage to follow the total number of stages throughout the optimization process, effectively eliminating the "variable overlap" problem, which departs from the commonly used methods in most existing studies.

4.0. Conclusion

In conclusion, we addresses two critical challenges related to the optimization of RED systems for ternary azeotropic mixtures. Our comprehensive analysis of existing studies highlighted a common emphasis on minimum cost (TAC) as the objective function and the utilization of various optimization algorithms and variables. Notably, the inclusion of reactive stages as optimization variables in most studies seems unnecessary, given that the EO hydration reaction is expected to occur throughout the entire column. This paper proposes a novel optimization procedure tailored for the RED system, specifically designed to overcome the "variable overlap" issue present in many existing methods. Our contribution aims to optimize the RED system more accurately, ensuring that reactive stages align with the total number of stages throughout the optimization process. While we do not claim to provide a global optimum, our innovative approach promises to yield refined RED designs that closely resemble real-world conditions. Our proposed optimization procedure is exemplified through two distinct case studies. In Case 1, we ventured into a scenario where the original process already designated a specific reaction zone. In this case, it is necessary to modify the original process so that the reaction can take place throughout the column, prior to optimizing it. Our analysis sought to unveil whether this adjustment would yield improved performance or potentially introduce adverse effects. Overall, it was found that the TAC of the optimized configuration increased by approximately 13% compared to the original case. This increase was due to the optimization approach that allowed the reaction to take place throughout the entire column, in contrast to the base case where it did not. In Case 2, we examined an alternative scenario where the reaction was distributed throughout the column without preceding optimization, and we noted only a slight reduction in TAC, approximately 3.87%. Overall, both optimized configurations offer a more precise and realistic approach that closely mimics real-world conditions. They address the "variable overlap" problem, departing from the commonly used methods in most existing studies.

Acknowledgments

Z. Kong gratefully acknowledged the support from Sunway University Malaysia. This project is also supported by the Sunway University Kick Start Grant Scheme (GRTIN-KSGS(02)-DEN-02-2023).

Data availability statement

All data generated or analysed during this study are available from the corresponding authors on reasonable request.

Nomenclature

Abbreviation

ACN	Acetonitrile
COM	Component object model
CY	Cyclohexane
DCRED	Double column reactive-extractive distillation
DDE	Dynamic Data Exchange
DE	Differential Evolution
DETL	Differential Evolution with Tabu List
DIPE	Diisopropyl ether (DIPE)
DWRED	Dividing-wall reactive-extractive distillation
EA	Ethyl acetate
ED	Extractive distillation

EG	Ethylene glycol
EO	Ethylene oxide
Eth	Ethanol
GA	Genetic algorithm
IPA	Isopropanol
MOGA	Multi-objective genetic algorithm
MOPSO	Multi-objective particle swarm optimization
NSGA-II	Non-dominated sorting genetic algorithm II
PSD	Pressure-swing distillation
PSO	Particle swarm optimization
RD	Reactive distillation
RED	Reactive-extractive distillation
REDC	Reactive-extractive distillation column
SIO	Sequential iterative optimization
SRC	Solvent regeneration column
SS-RED	Side-stream reactive-extractive distillation
TAC	Total annual cost
TBA	Tert-butyl alcohol

TCC	Total capital cost
TCRED	Three column reactive-extractive distillation
TC-RED	Thermally coupled reactive-extractive distillation
THF	Tetrahydrofuran
TL	Tabu list
TOC	Total operational cost

References

[1] Y. Su, A. Yang, S. Jin, W. Shen, P. Cui, J. Ren, Investigation on ternary system tetrahydrofuran/ethanol/water with three azeotropes separation via the combination of reactive and extractive distillation, J Clean Prod 273 (2020) 123145. https://doi.org/https://doi.org/10.1016/j.jclepro.2020.123145.

[2] A. Yang, W. Shen, S. Wei, L. Dong, J. Li, V. Gerbaud, Design and control of pressure-swing distillation for separating ternary systems with three binary minimum azeotropes, AIChE Journal 65 (2019) 1281–1293. https://doi.org/10.1002/aic.16526.

[3] C. Wang, Y. Zhuang, L. Liu, L. Zhang, J. Du, Design and comparison of energy-saving double column and triple column reactive-extractive hybrid distillation processes for ternary multi-azeotrope dehydration, Sep Purif Technol 259 (2021). https://doi.org/10.1016/j.seppur.2020.118211.

[4] T.-W. Wu, H.-C. Hua, C.-T. Kuo, I.-L. Chien, Novel Process Development of Hybrid Reactive–Extractive Distillation System for the Separation of a Cyclohexane/Isopropanol/Water Mixture with Different Feed Compositions, Ind Eng Chem Res 62 (2023) 2080–2089. https://doi.org/10.1021/acs.iecr.2c02889.

[5] J. Yan, J. Liu, J. Ren, Y. Wu, X. Li, T. Sun, L. Sun, Design and multi-objective optimization of hybrid reactive-extractive distillation process for separating wastewater containing benzene and isopropanol, Sep Purif Technol 290 (2022) 120915. https://doi.org/https://doi.org/10.1016/j.seppur.2022.120915.

[6] J. Huang, Q. Zhang, C. Liu, T. Yin, W. Xiang, Optimal design of the ternary azeotrope separation process assisted by reactive-extractive distillation for ethyl acetate/isopropanol/water, Sep Purif Technol 306 (2023) 122708. https://doi.org/https://doi.org/10.1016/j.seppur.2022.122708.

[7] Z.Y. Kong, J.G. Segovia-Hernández, H.-Y. Lee, J. Sunarso, Are process-intensified extractive distillation always energetically more efficient?, Chemical Engineering and Processing - Process Intensification 181 (2022) 109131. https://doi.org/https://doi.org/10.1016/j.cep.2022.109131.

[8] A. Yang, Z.Y. Kong, J. Sunarso, Design and optimisation of novel hybrid side-stream reactive-extractive distillation for recovery of isopropyl alcohol and ethyl acetate from wastewater, Chemical Engineering Journal 451 (2023) 138563. https://doi.org/https://doi.org/10.1016/j.cej.2022.138563.

[9] J. Liu, J. Yan, W. Liu, J. Kong, Y. Wu, X. Li, L. Sun, Design and multi-objective optimization of reactive-extractive dividing wall column with organic Rankine cycles considering safety, Sep Purif Technol 287 (2022) 120512. https://doi.org/https://doi.org/10.1016/j.seppur.2022.120512.

[10] Z.Y. Kong, J. Sunarso, A. Yang, Recent progress on hybrid reactive-extractive distillation for azeotropic separation: A short review, Frontiers in Chemical Engineering 4 (2022).

[11] Z.Y. Kong, E. Sánchez-Ramírez, A. Yang, W. Shen, J.G. Segovia-Hernández, J. Sunarso, Process intensification from conventional to advanced distillations: Past, present, and future, Chemical Engineering Research and Design 188 (2022) 378–392. https://doi.org/https://doi.org/10.1016/j.cherd.2022.09.056.

[12] Q. Zhao, X. Chu, Y. Li, M. Yan, X. Wang, Z. Zhu, P. Cui, Y. Wang, C. Wang, Economic, environmental, exergy (3E) analysis and multi-objective genetic algorithm optimization of isopropyl acetate production with hybrid reactive-extractive distillation, Sep Purif Technol 301 (2022) 121973. https://doi.org/https://doi.org/10.1016/j.seppur.2022.121973.

[13] Q. Zhao, Y. Li, C. Li, M. Yan, Z. Zhu, P. Cui, J. Qi, Y. Wang, C. Wang, Molecular dynamics-assisted process design and multi-objective optimization for efficient production of N-butyl acetate by reactive-extractive distillation/pervaporation, Sep Purif Technol 296 (2022) 121427. https://doi.org/https://doi.org/10.1016/j.seppur.2022.121427.

[14] Y. Cheng, B. Yang, G. Li, K. Chen, Z. Wei, X. Gao, H. Li, Z. Lei, Transesterification reactive extractive distillation process using ionic liquids as entrainers: From molecular insights to process integration, Sep Purif Technol 301 (2022) 122002. https://doi.org/https://doi.org/10.1016/j.seppur.2022.122002.

[15] Z.Y. Kong, A. Yang, C.-C. Tsai, V.S.K. Adi, A. Saptoro, J. Sunarso, Design and Optimization of Hybrid Reactive-Extractive Distillation for Ternary Azeotropic Separation: A Case Considering the Effect of Side Reactions, Ind Eng Chem Res 62 (2023) 10601–10610. https://doi.org/10.1021/acs.iecr.3c01532.

[16] C.-C. Tsai, Z.Y. Kong, A. Yang, V.S.K. Adi, J. Sunarso, A perspective on the inevitable side reactions in ethylene-glycol based reactive-extractive distillation, Chemical Engineering Journal 475 (2023) 146331. https://doi.org/https://doi.org/10.1016/j.cej.2023.146331.

[17] Y.R. Zhang, T.W. Wu, I.L. Chien, Intensified hybrid reactive-extractive distillation process for the separation of water-containing ternary mixtures, Sep Purif Technol 279 (2021). https://doi.org/10.1016/j.seppur.2021.119712.

[18] A. Yang, Y. Su, S. Sun, W. Shen, M. Bai, J. Ren, Towards sustainable separation of the ternary azeotropic mixture based on the intensified reactive-extractive distillation configurations and multi-objective particle swarm optimization, J Clean Prod 332 (2022). https://doi.org/10.1016/j.jclepro.2021.130116.

[19] Y. Li, T. Sun, Q. Ye, J. Li, Y. Xu, X. Jian, Economic and environmental assessment for purification of acetonitrile and isopropanol by reactive coupling extractive distillation, Sep Purif Technol 275 (2021) 119133. https://doi.org/https://doi.org/10.1016/j.seppur.2021.119133.

[20] Z.Y. Kong, A. Yang, J. Chua, J.J. Chew, J. Sunarso, Energy-Efficient Hybrid Reactive-Extractive Distillation with a Preconcentration Column for Recovering Isopropyl Alcohol and Diisopropyl Ether from Wastewater: Process Design, Optimization, and Intensification, Ind Eng Chem Res 61 (2022) 11156–11167. https://doi.org/10.1021/acs.iecr.2c01768.

[21] Z.Y. Kong, G.C. Zarazúa, H.-Y. Lee, J. Chua, J.G. Segovia-Hernández, J. Sunarso, Design of novel side-stream hybrid reactive-extractive distillation for sustainable ternary separation of THF/ethanol/water using mixed entrainer, Process Safety and Environmental Protection 166 (2022) 574–588. https://doi.org/https://doi.org/10.1016/j.psep.2022.08.056.

[22] X. Geng, P. Yan, H. Zhou, H. Li, X. Gao, Process synthesis and 4E evaluation of hybrid reactive distillation processes for the ethanol and tert-butanol recovery from wastewater, Renew Energy 205 (2023) 929–944. https://doi.org/https://doi.org/10.1016/j.renene.2023.01.107.

[23] Z.Y. Kong, A. Yang, C.-C. Tsai, V.S.K. Adi, A. Saptoro, J. Sunarso, Design and Optimization of Hybrid Reactive-Extractive Distillation for Ternary Azeotropic Separation: A Case Considering the Effect of Side Reactions, Ind Eng Chem Res 62 (2023) 10601–10610. https://doi.org/10.1021/acs.iecr.3c01532.

[24] C. Wang, Y. Zhuang, Y. Qin, Y. Dong, L. Liu, L. Zhang, J. Du, Design and eco-efficiency analysis of sustainable extractive distillation process combining preconcentration and solvent recovery functions for separating the tetrahydrofuran/ethanol/water ternary multi-azeotropic mixture, Process Safety and Environmental Protection 159 (2022) 795–808. https://doi.org/https://doi.org/10.1016/j.psep.2022.01.060.

[25] C. Wang, Y. Zhuang, Y. Qin, Y. Dong, L. Liu, L. Zhang, J. Du, Optimization and eco-efficiency analysis of extractive distillation processes with different solvents for separating the ternary mixture embedding two azeotropes, Sep Purif Technol 269 (2021) 118763. https://doi.org/https://doi.org/10.1016/j.seppur.2021.118763.

[26] Bilal, M. Pant, H. Zaheer, L. Garcia-Hernandez, A. Abraham, Differential Evolution: A review of more than two decades of research, Eng Appl Artif Intell 90 (2020) 103479. https://doi.org/https://doi.org/10.1016/j.engappai.2020.103479.

[27] S. Chakraborty, A.K. Saha, A.E. Ezugwu, J.O. Agushaka, R.A. Zitar, L. Abualigah, Differential Evolution and Its Applications in Image Processing Problems: A Comprehensive Review, Archives of Computational Methods in Engineering 30 (2023) 985–1040. https://doi.org/10.1007/s11831-022-09825-5.

[28] M. Srinivas, G.P. Rangaiah, Differential Evolution with Tabu List for Solving Nonlinear and Mixed-Integer Nonlinear Programming Problems, Ind Eng Chem Res 46 (2007) 7126–7135. https://doi.org/10.1021/ie070007q.

[29] M. Srinivas, G.P. Rangaiah, Differential Evolution with Tabu List for Global Optimization: Evaluation of Two Versions on Benchmark and Phase Stability Problems, in: Differential Evolution in Chemical Engineering, World Scientific, 2016: pp. 91–127. https://doi.org/doi:10.1142/9789813207523_0004.

[30] E. Sánchez-Ramírez, B. Huerta-Rosas, J.J. Quiroz-Ramírez, V.A. Suárez-Toriello, G. Contreras-Zarazua, J.G. Segovia-Hernández, Optimization-based framework for modeling and kinetic parameter estimation, Chemical Engineering Research and Design 186 (2022) 647–660. https://doi.org/https://doi.org/10.1016/j.cherd.2022.08.040.

[31] J.A. Vázquez-Castillo, G. Contreras-Zarazúa, J.G. Segovia-Hernández, A.A. Kiss, Optimally designed reactive distillation processes for eco-efficient production of ethyl levulinate, Journal of Chemical Technology & Biotechnology 94 (2019) 2131–2140. https://doi.org/https://doi.org/10.1002/jctb.6033.

[32] K. Guthrie, Capital cost estimating, Chemical Engineering 76 (1969) 114–142.

[33] G.D., J.W.& S.N.Y.C.B.T.S. "1984" 472 pages. $35. 95 Ulrich, A guide to chemical engineering process design and economics, John Wiley & Sons, Ltd, 1984. https://doi.org/https://doi.org/10.1002/aic.690300636.

[34] R. Turton, R.C. Bailie, W.B. Whiting, J.A. Shaeiwitz, Analysis, Synthesis and Design of Chemical Processes, Pearson Education, 2008.

[35] Y.C. Wu, P.H.C. Hsu, I.L. Chien, Critical assessment of the energy-saving potential of an extractive dividing-wall column, Ind Eng Chem Res 52 (2013) 5384–5399. https://doi.org/10.1021/ie3035898.

[36] Y.C. Wu, H.Y. Lee, H.P. Huang, I.L. Chien, Energy-saving dividing-wall column design and control for heterogeneous azeotropic distillation systems, Ind Eng Chem Res 53 (2014) 1537–1552. https://doi.org/10.1021/ie403136m.

.

.

CRediT authorship contribution statement

Eduardo Sánchez-Ramírez: Methodology, Resources, Software, Validation, Visualization, Writing - original draft, Writing - review & editing. **Shirui Sun:** Validation, Writing - original draft, Writing - review & editing. **Jia Yi Sim:** Data curation, Investigation, Visualization, Writing – original draft, Writing - review & editing. **Ao Yang:** Formal analysis, Writing - original draft, Writing - review & editing. **Zong Yang Kong:** Conceptualization, Data curation, Formal analysis, Project administration, Supervision, Visualization, Writing - original draft, Writing - review & editing, Funding acquisition. **Juan Gabriel Segovia-Hernández:** Methodology, Project administration, Resources, Software, Writing - original draft, Writing - review & editing.

Highlights

- Omission of reactive stage as optimization variables
- Provides a more realistic approach for optimizing reactive-extractive distillation
- Allow ethylene oxide reaction to take place throughout the column
- Align total stages with reactive stages during optimization process

Declaration of interests

☒ The authors declare that they have no known competing financial interests or personal relationships that could have appeared to influence the work reported in this paper.

☐ The authors declare the following financial interests/personal relationships which may be considered as potential competing interests: